NUMERICAL SIMULATION OF NON-CONVENTIONAL LIQUID FUELS FEEDING IN A BUBBLING FLUIDIZED BED COMBUSTOR

by

Milica R. MLADENOVIĆ [a]*, Stevan Dj. NEMODA [a], Mirko S. KOMATINA [b], and Dragoljub V. DAKIĆ [c]

[a] Laboratory for Thermal Engineering and Energy, Vinča Institute of Nuclear Sciences, University of Belgrade, Belgrade, Serbia
[b] Faculty of Mechanical Engineering, University of Belgrade, Belgrade, Serbia
[c] Innovation Centre, Faculty of Mechanical Engineering, University of Belgrade, Belgrade, Serbia

Original scientific paper
DOI: 10.2298/TSCI121116007M

The paper deals with the development of mathematical models for detailed simulation of lateral jet penetration into the fluidized bed, primarily from the aspect of feeding of gaseous and liquid fuels into fluidized bed furnaces. For that purpose a series of comparisons has been performed between the results of in-house developed procedure – fluid-porous medium numerical simulation of gaseous jet penetration into the fluidized bed, Fluent's two-fluid Euler-Euler fluidized bed simulation model, and experimental results (from the literature) of gaseous jet penetration into the 2-D fluidized bed. The calculation results, using both models, and experimental data are in good agreement. The developed simulation procedures of jet penetration into the fluidized bed are applied to the analysis of the effects, which are registered during the experiments on a fluidized pilot furnace with feeding of liquid waste fuels into the bed, and brief description of the experiments is also presented in the paper. Registered effect suggests that the water in the fuel improved mixing of fuel and oxidizer in the fluidized bed furnace, by increasing jet penetration into the fluidized bed due to sudden evaporation of water at the entry into the furnace. In order to clarify this effect, numerical simulations of jet penetration into the fluidized bed with three-phase systems: gas (fuel, oxidizer, and water vapour), bed particles and water, have been carried out.

Key words: *numerical simulation, fluidized bed, jet penetration, two-fluid Euler-Euler model*

Introduction

For the purpose of developing an environmentally friendly technology for incineration of crude-oil sludge and other waste materials with the characteristics of low grade fuels, in the Laboratory for Thermal Engineering and Energy of the Vinča Institute of Nuclear Sciences research is currently being done on the development of fluidized bed technology for combustion of non-conventional solid and liquid fuels, *i. e.* industrial waste materials. To this aim, a series of measurements was done on a semi-industrial experimental fluidized bed (FB) facility with combustion of high density and viscosity liquid fuels, as well as on the demonstrative experimental hot water FB boiler (with the capacity of about 500 kW).

Benefits of combusting unconventional fuels (with high contents of water and other ballast substances) in a FB are numerous. Primarily, high heat capacity and thermal conductivity

* Corresponding author; e-mail: mica@vinca.rs

of the bed, and intense heat transfer between particles of inert bed material and the fuel, enables a stable combustion process of a wide range of non-conventional fuels, with low sensitivity to changes in fuel quality. The zone of intense combustion occupies a relatively small volume, because most of the fuel is burned in the bed itself, with post-combustion of a small fuel part in the "splash" zone and above the bed. In addition, the FB facilities usually operate at temperatures of about 850 °C which are optimal from the aspect of the reduced concentration of NO_x compounds in the flue gases. Also, these furnaces are favourable from the aspect of desulphurization efficiency by adding limestone into the furnace [1], when it is necessary. For all these reasons this technology is recommended by the EU for the combustion of waste materials.

For the purpose of investigation in energy and process engineering, besides the experimental methods, application of numerical simulation is becoming more and more often. Its advantages are in savings of means and time for the development of facilities and technologies in this field.

The most common numerical models for simulation of FB processes can be classified as Lagrangian models [2, 3], where each particle, *i. e.* representative of a characteristic group of particles, is tracked numerically during its motion within the FB; or as Eulerian models, where focus are on specific regions of the flow domain, through which gas or particles flows. Lagrangian approach to the simulation of particle motion in the FB is more exact, but Eulerian FB modeling approach provides relatively simpler numerical solutions and is therefore more used in engineering practice. The so-called two-fluid FB modeling procedure is of special importance [4, 5], where gas and dense phase of the FB (gas-particles system at conditions of minimal fluidization) are considered as two fluids with different characteristics. In momentum conservation equations for an effective fluid (representing the dense phase of the FB), fluid-particle interaction at conditions of minimal fluidization is modeled, as well as interaction between the particles themselves.

One of the two numerical models this work suggests is a simplified version of a two-fluid model previously developed in-house, where the FB dense phase is considered as a fixed porous medium [6]. Gas-particle interactions, as well as conditions for occurrence of bubbles and non-particle zones, are modeled in a similar way as in the case of two-fluid models, except that the simulation of particle motion, *i. e.* dense phase, is excluded.

The second method of numerical simulation of FB processes, used in this paper, is the Euler-Euler granular model, where a professional CFD code (FLUENT 6.3.26) are applied for modeling the interaction between the fluid and granular particles of the fluidized bed.

The calculation results, using both proposed models, have been compared with experimental results from the literature, in which a series of measurements of penetration length of a lateral gas jet into the 2-D FB is carried out, with the help of a camcorder [7].

The developed simulation procedures of jet penetration into the FB have been applied to the analysis of the effect, which are registered in the experiments on the FB pilot facility with feeding of liquid fuel into the bed, when moving of the intense combustion zone towards areas deeper below the FB surface was noticed during the combustion of liquid fuels with significant water contents (when compared to moisture-free fuel). The observed effect leads to the conclusion that water in the fuel increases the global reaction rate of combustion in the FB furnace with lateral fuel feeding into the fluidized bed. This phenomenon was observed both with liquid fuels of high and low volatility (more and less evaporative liquid fuels, respectively), and can be explained by the increase of the volumetric flow of the fuel jet fed into the bed, due to the transition of water from the fuel into steam. In order to clarify this effect, numerical simulations of jet penetration into the FB were carried out for three-phase systems consisting of: gas (fuel, oxidizer,

and water vapour), bed particles and water, which at the nozzle outlet transforms into steam. The case of combustion of light volatile fuels was analyzed by simulating the penetration of a jet containing volatile fuel components and water in liquid state (which rapidly evaporates in the furnace), while the case of heavy volatile fuel was considered by simulating a jet with a mixture of oil and water. These calculations are unsteady (non-stationary) and they model the first moments of jet formation.

Two-fluid CFD models of fluidization

As it was already mentioned in the introduction, two methods of CFD simulations of the FB in accordance with the two-fluid modeling approach are proposed. The models have been applied to the case of lateral penetration of a gas jet into a 2-D FB, and the calculation results have been compared with experimental results from the literature.

Fluid-porous medium model of the FB

As the majority of two-fluid models, the suggested numerical model of the FB is based on the assumptions of Davidson's [8] two-phase fluidization model. According to the suggested model, the gas flow through the particle (dense) phase and through bubble zones (non-particle zones) is observed. The volumetric zones with and without particles are defined on the basis of the gas-particle phase interaction model. The non-particle zones (bubbles) are considered as turbulent gas flows, while the dense phase is modeled in accordance with flow models through porous media.

The flow in the FB is described by momentum conservation equations for turbulent flow, in conjunction with the continuity equation, with the correction of pressure drop for particle-containing zones under conditions of minimum fluidization velocity (dense phase of the FB). In common models of flow through a porous media, the flow is assumed to be laminar, because of a very narrow space for fluid passage between the particles. However, in addition to the non-particle zones (bubbles), it is assumed that turbulent flow is present in dense phase regions as well, because the particles at minimum fluidization velocity are in the state of chaotic motion, and hence turbulent fluid flow can be assumed between them. Prediction of the positions and sizes of bubble-zones (*i. e*. non-particle zones) is modeled by setting the balance of friction forces between the particles and the fluid, taking into account the forces of inter-particle interactions.

All the calculations are stationary, hence the model offers the possibility to obtain an average image of the flow in the FB with locations and shapes of the most frequently detected non-particle zones.

The main conservation equations, given in tensor notation, are:

– continuity equation

$$\frac{\partial}{\partial x_j}(\rho U_j) = 0 \tag{1}$$

– momentum transfer equation for the gas phase in *i*-direction

$$\frac{\partial}{\partial x_j}(\rho U_j U_i) - \frac{\partial}{\partial x_j}\left(\mu_{\text{eff}} \frac{\partial U_i}{\partial x_j}\right) = -\frac{\partial p}{\partial x_i} + \frac{\partial}{\partial x_j}\left(\mu_{\text{eff}} \frac{\partial U_j}{\partial x_i}\right) - \frac{2}{3}\frac{\partial}{\partial x_i}\left(\mu_{\text{eff}} \frac{\partial U_k}{\partial x_k}\right) \tag{2}$$

– momentum transfer equation for the dense phase in *i*-direction

$$\frac{\partial}{\partial x_j}(\rho U_j U_i) - \frac{\partial}{\partial x_j}\left(\mu_{\text{eff}} \frac{\partial U_i}{\partial x_j}\right) =$$

$$= -\frac{\partial p}{\partial x_i} - \left(\frac{\mu}{K_{1,j}} U_j + \frac{\rho}{K_{2,j}} U_j |U_j|\right) + \frac{\partial}{\partial x_j}\left(\mu_{\text{eff}} \frac{\partial U_j}{\partial x_i}\right) - \frac{2}{3}\frac{\partial}{\partial x_i}\left(\mu_{\text{eff}} \frac{\partial U_k}{\partial x_k}\right) \quad (3)$$

Turbulent viscosity is determined from the k-ε turbulence model as $\mu_t = C\mu\rho k^2/\varepsilon$, where $\mu_{\text{eff}} = \mu + \mu_t$ is the effective viscosity. The turbulent energy and turbulent energy dissipation (k and ε) equations are defined in [10].

The additional term in the momentum transport equation, in the zones with the dense phase, is modeled in accordance with the Forchheimer's equation:

$$\frac{\partial p}{\partial x_i} = -\frac{\mu}{K_{1,i}} U_j - \frac{\rho}{K_{2,i}} |U_j| U_j \quad (4)$$

Tensors $K_{1,i}$ and $K_{2,i}$ are linear and turbulent permeability coefficients, respectively. These coefficients, for FB dense phase conditions, are defined according to the Ergun's equation as:

$$K_{1,i} = \frac{\alpha_g^3 d_p^2}{150(1-\alpha_g)^2}, \quad K_{2,i} = \frac{\alpha_g^3 d_p^2}{1.75(1-\alpha_g)} \quad (5)$$

Gas-particles interaction forces, similar to more complex two-fluid models, can be reduced to the force of friction between the gas and particles in the FB dense phase, and are defined according to the Ergun's equation, eqs. (4) and (5). Interactions between particles can be reduced to the inter-particle friction force and to the effects of inter-particle collisions in the FB. These two effects are modeled together, using the expression for the effective inter-particle friction force: $F_p = \psi_{fr}\rho_b(1-\alpha_g)g$. Term $\rho_b(1-\alpha_g)$ refers to the pressure of the deposited bed of particles over bed differential height, and ψ_{fr} is the effective friction coefficient of the bed particles, which at the same time refers to the effects of collision between the fluidized bed particles and is defined by the following semi-empirical expression: $\psi_{fr} = \alpha(U_s/U_{mf})^b$. The constants a and b are the only empirical constants of the proposed model, and in accordance with experimental verification, shown in [6], adopted values are 0.65 and 1.5, respectively.

Euler-Euler granular model of the fludized bed

Euler-Euler fluidized bed modeling approach assumes that the gas and FB dense phase (gas-particle system under conditions of minimum fluidization) are considered as two fluids with different characteristics. In the transport equations for transfer of momentum of the effective fluid, which is the FB dense phase, fluid-particle interactions in conditions of minimum fluidization velocity are modeled, as well as the interaction between the particles themselves. In the Eulerian-Eulerian approach all phases have the same pressure and that is the pressure of the continuous-primary phase. This model solves the continuity and momentum equations, for each phase, and tracks the volume fraction – $\alpha_k = V_k/V$, $1 = \Sigma\alpha_k$, $k = g, s$. Further, an additional transport equation for the granular temperature (which represents the solids fluctuating energy) is solved, as well as the solids bulk and shear viscosity, which is determined using the kinetic theory of gases on granular flow. It is also necessary to define the coefficients for calculating the inter-phase interaction term. Turbulence model (k-ε) can be applied to all phases.

For modeling the interactions between gas and particle phases, within the suggested Euler-Euler granular approach to fluidized bed modeling, the routines incorporated in the mod-

ules of the commercial CFD software package FLUENT 6.3.26 have been used. This code allows the presence of several phases within one control volume of the numerical grid, by introducing the volume fraction of each phase. The solid phase represents a granular layer made of spherical particles, with uniform diameters. Mass and momentum conservation equations are solved for each phase separately.

The basic and constitutive equations of the two-fluid granular model of the fluidized bed can be described by the set of expressions [11]:

– continuity equation of the gas phase

$$\frac{\partial}{\partial t}(\alpha_g \rho_g) + \nabla(\alpha_g \rho_g \vec{u}_g) = 0 \tag{6}$$

– continuity equation of the solid phase

$$\frac{\partial}{\partial t}(\alpha_s \rho_s) + \nabla(\alpha_s \rho_s \vec{u}_s) = 0 \tag{7}$$

– momentum conservation equation of the gas phase

$$\frac{\partial}{\partial t}(\alpha_g \rho_g \vec{u}_g) + \nabla(\alpha_g \rho_g \vec{u}_g \vec{u}_g) = -\alpha_g \nabla p + \nabla \boldsymbol{\tau}_g + \alpha_g \rho_g \vec{g} + K_{gs}(\vec{u}_g - \vec{u}_s) \tag{8}$$

– momentum conservation equation of the solid phase

$$\frac{\partial}{\partial t}(\alpha_s \rho_s \vec{u}_s) + \nabla(\alpha_s \rho_s \vec{u}_s \vec{u}_s) = -\alpha_s \nabla p + \nabla \boldsymbol{\tau}_s + \alpha_s \rho_s \vec{g} + K_{gs}(\vec{u}_g - \vec{u}_s) \tag{9}$$

The stress tensor of the gas and the granular phases are, respectively:

$$\boldsymbol{\tau}_g = 2\mu_g \mathbf{S}_g + \left(\lambda_g - \frac{2}{3}\mu_g\right)\nabla \vec{u}_g [\mathbf{I}]$$

$$\boldsymbol{\tau}_s = -p_s[\mathbf{I}] + 2\alpha_s \mu_s \mathbf{S}_s + \alpha_s\left(\lambda_s - \frac{2}{3}\mu_s\right)\nabla \vec{u}_s [\mathbf{I}]$$

where $\mathbf{S}_k = 1/2[\nabla \vec{u}_k + (\nabla \vec{u}_k)^T]$, $k = g, s$ is the strain rate tensor, $p_s = 2\rho_s \Theta_s (1 + e_s)\alpha_s^2 g_{0s}$ is the pressure of the granular phase [12], while g_{0s} is a radial distribution function, which for Syamlal model is equal to $g_0(\alpha_s) = 1/(1 - \alpha_s) + 3\alpha_s/2(1 - \alpha_s)^2$, and e_s is the restitution coefficient.

Solids bulk viscosity λ_s is a measure of resistance of solid particles to expansion/compression and according to Lun *et al*. model [13] is defined as: $\lambda_s = 4/3\alpha_s d_s g_{os}(1 + e_s)(\Theta_s/\pi)^{0.5}$

Viscosity of the granular phase consists of solids shear viscosity μ_s and bulk viscosity λ_s. Shear viscosity is the result of translator motion (kinetic viscosity $\mu_{s,kin}$), mutual particle collisions (collision viscosity $\mu_{s,coll}$) and frictional viscosity ($\mu_{s,fr}$): $\mu_s = \mu_{s,kin} + \mu_{s,coll} + \mu_{s,fr}$.

According to the Syamlal model [12], the kinetic viscosity is:
$\mu_{s,kin} = [\alpha_s d_s \rho_s (\Theta_s \pi)^{0.5}/12(2 - \eta)][1 + (8/5)\eta(3\eta - 2)\alpha_s g_{0s}]$, $\eta = (1 + \alpha_s)/2$, and for the collisional viscosity following expression applies: $\mu_{s,coll} = (8/5)\alpha_s \rho_s d_s g_{0s} \eta (\Theta_s/\pi)^{0.5}$. According to Schaeffer's model [14] frictional viscosity could be defined as: $\mu_{s,fr} = p_s \sin\phi/2(\mathbf{I}_{2D})^{0.5}$, where p_s is the granular phase (solids) pressure, ϕ – the angle of internal friction for the particle, and $\mathbf{I}_{2D}$ – the second invariant of the deviator of the strain rate tensor.

The last term of the eqs. (8) and (9) is a consequence of the inter-phase interaction drag force, where the coefficient between fluid and solid (granular) phase, according to the Syamlal-O'Brien model [15], is:

$$K_{\mathrm{gs}} = \frac{3\alpha_{\mathrm{g}}\alpha_{\mathrm{s}}\rho_{\mathrm{g}}}{4u_{r,s}^2 d_{\mathrm{s}}} C_{\mathrm{D}} |\vec{\mathrm{u}}_{\mathrm{s}} - \vec{\mathrm{u}}_{\mathrm{g}}|, \quad C_D = \left(0.63 + \frac{4.8}{\sqrt{\frac{\mathrm{Re}_{\mathrm{s}}}{u_{\mathrm{r,s}}}}} \right)^2, \quad \mathrm{Re}_{\mathrm{s}} = \frac{\rho_g d_{\mathrm{s}} |\vec{\mathrm{u}}_{\mathrm{s}} - \vec{\mathrm{u}}_{\mathrm{g}}|}{\mu_{\mathrm{g}}}$$

Terminal velocity of particles in fluidized bed $u_{\mathrm{r,s}}$ is determined as:

$$u_{\mathrm{r,s}} = 0.5[A - 0.06\,\mathrm{Re}_{\mathrm{s}} + \sqrt{(0.06\,\mathrm{Re}_{\mathrm{s}})^2 + 0.12\,\mathrm{Re}_{\mathrm{s}}(2B - A) + A^2}$$

$$A = \alpha_g^{4.14}, \quad B = \begin{cases} = 0.8\alpha_g^{1.28} & \text{for} \quad \alpha_g \le 0.85 \\ = \alpha_g^{2.65} & \text{for} \quad \alpha_g > 0.85 \end{cases}$$

Granular temperature, starting from the equations of conservation of fluctuating granular energy, is:

$$\frac{3}{2}\left[\frac{\partial}{\partial t}(\rho_{\mathrm{s}}\alpha_{\mathrm{s}}\Theta_{\mathrm{s}}) + \nabla(\rho_{\mathrm{s}}\alpha_{\mathrm{s}}\vec{\mathrm{u}}_{\mathrm{s}}\Theta_{\mathrm{s}}) \right] = (-\rho_{\mathrm{s}}[\mathbf{I}] + \boldsymbol{\tau})_{\mathrm{s}} : \nabla\vec{\mathrm{u}}_{\mathrm{s}} + \nabla(k_{\Theta_{\mathrm{s}}}\nabla\Theta_{\mathrm{s}}) - \gamma_{\Theta_{\mathrm{s}}} + \phi_{\mathrm{gs}}$$

The diffusion coefficient or conductivity of granular temperature, according to Syamlal [12], is:

$$k_{\Theta_{\mathrm{s}}} = \frac{15\alpha_{\mathrm{s}}\rho_{\mathrm{s}}d_{\mathrm{s}}\sqrt{\Theta_{\mathrm{s}}\pi}}{4(41 - 33\eta)}\left[1 + \frac{12}{5}\alpha_{\mathrm{s}}g_{\mathrm{os}}\eta^2(4\eta - 3) \right]$$

Granular energy dissipation due to inelastic collisions, Lun *et al*. [13] define as: $\gamma_{\Theta_{\mathrm{s}}} = [12(1 - e_{\mathrm{s}})\mathrm{g}_{\mathrm{os}}/d_{\mathrm{s}}(\pi)^{1/2}]\rho_{\mathrm{s}}\alpha_{\mathrm{s}}\Theta_s^{3/2}$. Exchange of kinetic energy between the phases is determined by: $\phi_{\mathrm{gs}} = -3K_{\mathrm{gs}}\Theta_{\mathrm{s}}$.

Comparison of the proposed models with the experiments

Proposed methods of numerical simulation of the fluidized bed are primarily applied to the case of determining the penetration length of the lateral gas jet into a 2-D layer/bed of particles fluidized by air, as a function of the velocity of the fluid at the exit of the horizontal nozzle. Parenthetically, this analysis is very useful in trying to find the solutions for combustion of liquid and gaseous fuel in the FB reactor, whereby the numerical method enables a rapid and relatively simple analysis of possible technical solutions for injection of fuels with preferred heat capacities into the FB reactor, achieving at the same time more efficient mixing with bed inert material.

Primarily in order to verify the proposed CFD models, the results of in-house developed procedure of fluid-porous medium simulation of the penetration of the gaseous jet into the FB and Fluent's two-fluid Euler-Euler FB simulation model have been compared to the results of extensive experimental investigations of the penetration of a lateral air jet into the 2-D FB [7].

Experiments were conducted on a Plexiglas set-up with a two-dimensional FB, 314 mm wide and 25 mm thick, with the possibility to change the position and the inclination of the lateral jet. The lateral jet penetration length into the FB was measured by a camcorder, with the

photo-shooting frequency of 25 pictures per second. The measurement error for the jet penetration length, obtained by this procedure, was not higher than 5 mm.

Based on the experimental results, in [7] a semi-empirical dependence correlation of the horizontal jet penetration length into the FB as a function of fluidization parameters and nozzle characteristics is proposed:

$$\frac{L_j}{d_j} = 1.89 \cdot 10^6 \left[\frac{\rho_j U_j^2}{(1-\varepsilon_b)\rho_s g d_p} \right]^{0.327} \left(\frac{\rho_f}{\rho_s} \right)^{1.974} \left(\frac{d_p}{d_:} \right)^{-0.04} - 3.8 \qquad (10)$$

Numerical solving of own fluid-porous medium model equations, defined by the expressions (1-5), has been performed by using the control volume method [10], including the collocated numerical grid for momentum equations, hybrid numerical scheme (with the combination of upstream and central differencing) and SIMPLE algorithm for solving the equations [10]. Differential equations are non-linear and mutually coupled. The iteration process stabilization is done by sub-relaxation technique. The calculation procedure and the numerical method are described in more details in [9]. The numerical grid shown in fig. 1, consisting of 9604 nodes, was used. A test calculations for the purposes of this model showed that using numerical grid with a larger number of nodes does not give significant changes to the calculation results. The whole calculation area covers the area of the fluidized bed with the presence of bubbles and dense phase, the distribution of which is determined in accordance with the proposed model. A uniform distribution of fluidization air has been assumed.

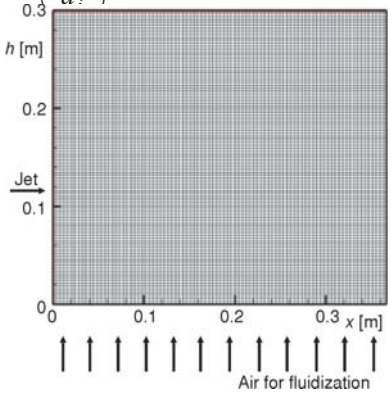

Figure 1. Fluid-porous medium model scheme of the numerical grid and boundary conditions

Numerical solving of the governing equations of Fluent's Euler-Euler granular model (eq. 9-11), is also performed by the method of control volumes whereby the coupling and correction of the velocity and pressure is carried out for multiphase flows with the Phase Coupled SIMPLE (PCSIMPLE) algorithm. The discretisation of the convective terms was carried out with the second-order upwind scheme. Calculations are non-stationary, with a time step of $2.5 \cdot 10^{-4}$ s, which allowed a relatively quick convergence with a maximum of 100 iterations per time step, where the convergence criterion between two iterations was set to $1 \cdot 10^{-3}$.

The number of time steps, *i. e.* the total simulation time, has been determined by the time required for the fluid to pass through the space occupied by FB. The computational domain geometry is shown in fig. 2. Numerical grid consists of 14700 nodes in total whereby

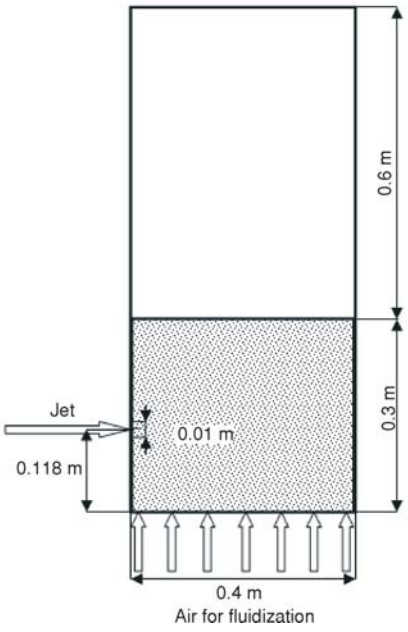

Figure 2. The workspace of the two-fluid granular model of the FB

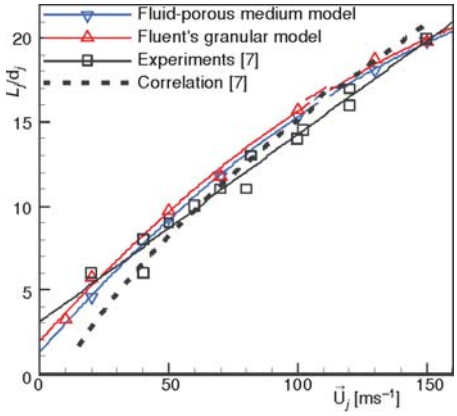

Figure 3. Results of the comparison of two numerical models with experimental results [7] and semi-empirical correlation [7]

fluidized bed zone contains 9800 nodes and the zone above – freeboard surface contains 4900 nodes. Statistical analysis of non-stationary calculations has been performed by forming and installation of specialized subroutines in the "C" programming language ("user defined functions"), wherewith the user is able to upgrade individual parts of the core Fluent's code.

The comparison of the computer simulation of jet penetration length as a function of air velocity in the nozzle, with the experimental results from [7], is shown in fig. 3. The results of the numerical calculation obtained both by the FB fluid-porous medium model and by the Fluent granular model, are in very good agreement with each other and with experimental data and correlation (10). In fig. 4, a comparison is shown of numerically obtained dependence of dimensionless horizontal jet penetration distance and the jet velocity at the entrance to the FB, with the experimental results and those obtained using the semi-empirical correlation of some other authors [16-21].

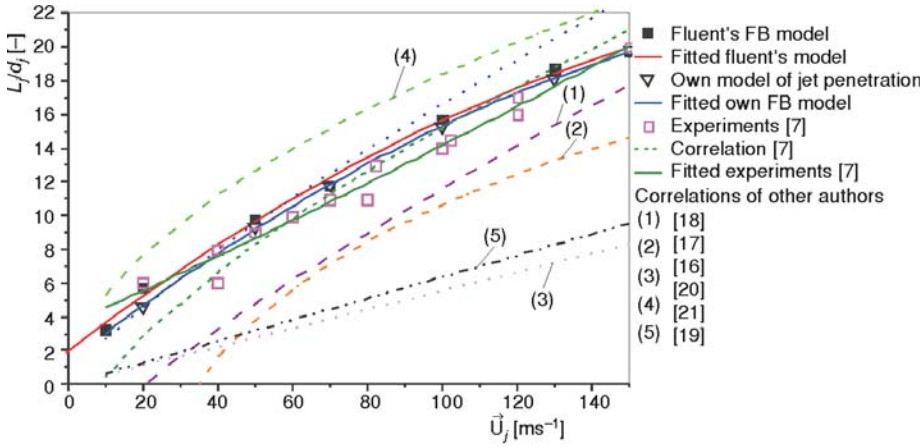

Figure 4. Comparison of the proposed models with experimental data and semi empirical correlations of some other authors

The simulation of the development of horizontal jet in time, using Fluent's two-fluid Euler-Euler granular model of the fluidized bed, is shown in fig. 5. A horizontal airflow jet with the velocity of 20 m/s is introduced at the height of 0.118 m into the fluidized bed, with particle diameter of 0.00143 m and density of 1402 kg/m^3. The fluidization number is $N = 3$, and the height and the width of the bed are 0.3 m and 0.4 m, respectively. The bed voidage implies void fraction of fluid/gas phase.

Figure 5, as an illustration, displays more detailed just one of the series of numerical experiments of the lateral jet development in FB, based on which is drawn a diagram in fig. 3. To

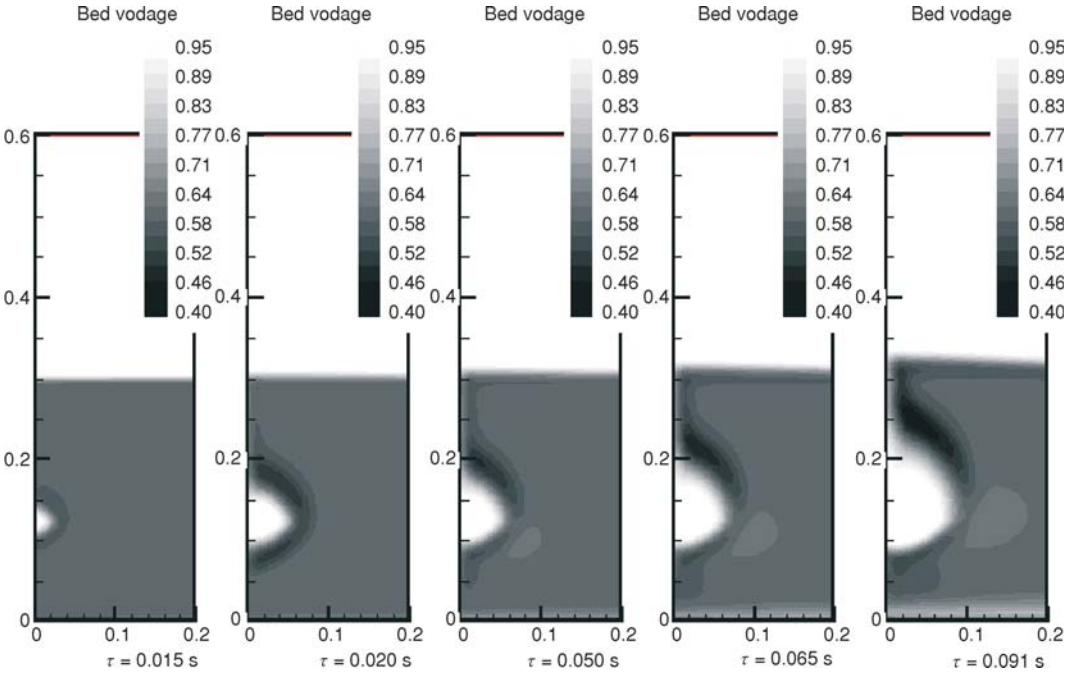

Figure 5. Simulation of the development of a horizontal jet (with the velocity of 20 m/s) with time, using a two-fluid granular model of the FB

determine the exact length of the lateral jet penetration in each time interval, a special subroutine has been made, which is incorporated by UDF in Fluent's code.

Experiments on pilot furnace with liquid fuel feeding into the FB

Effect of withdrawal of the intense combustion zone towards the areas below the bed surface during the combustion of liquid fuels with significant water content, compared to those without moisture or with low moisture content, was investigated on the semi-industrial experimental fluidized bed installation with the liquid fuel feeding system. The experimental set-up is shown in details in the papers [22-24]. To confirm the aforementioned, in this chapter brief analysis of fluidized bed combustion results for waste grease from the cold rolling mill USS (Smederevo, Serbia) are given. The accent has been put on the dependence of temperature change with furnace height on the characteristics of the fuel, *i. e.* the water content in it.

The fuel examined was combusted in the fluidized bed in three steady regimes:

– Regime I – fuel as delivered, without addition of water,
– Regime II – fuel/water mixture in the ratio (60:40)% volume fraction, and
– Regime III – fuel/water mixture in the ratio (50:50)% volume fraction.

Bed material was quartz sand with average diameter $d_p = 0.8$ mm and bulk density $\rho_b = 1585$ kg/m^3. The bed height was $H_o = 371$ mm. The fuel was homogenized by continuous mixing and heated up to 70 °C. Jet nozzle immersion depth into the bed h in all regimes was such that the valid ratio was $H_o - h = 0.7\,H_o$, where h is the distance between the top of the submerged fuel nozzle and the top of air distributor nozzles, and H_o is the bed static height measured from the top of distributor. Output diameter of the nozzle is $d_j = 12$ mm.

Table 1. Proximate analysis of analytical sample

Moisture	%	13.21
Ash	%	2.27
Sulfur total	%	0.72
Char	%	2.78
C-fix	%	0.51
Volatile matter	%	84.01
Combustible matter	%	84.52
HHV	kJ	32133
LHV	kg	29791

Proximate analyses of analytical sample of grease from the cold rolling mill are given in tab. 1.

As it can be observed from the fig. 6, temperatures within the bed are almost equal, and the temperature immediately by the freeboard of the expanded bed does not differ much from temperatures within the bed by which stable process is achieved. The intense combustion zone in all three regimes is located above the freeboard, especially in regime I (see fig. 6), meaning that bubbles filled with fuel fumes and air leave the bed before fuel combustion within the bubbles is completed. On the other hand, by mixing the fuel with water, in regimes II and III, decreasing of temperature differences in the bed and immediately above the bed can be noticed (fig. 6.).

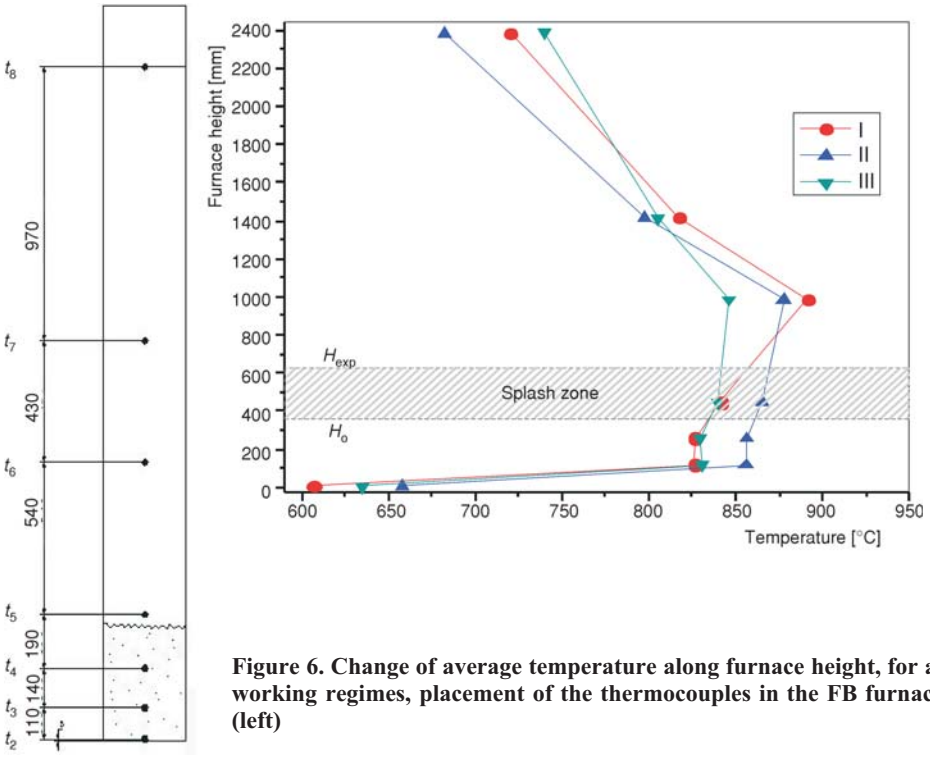

Figure 6. Change of average temperature along furnace height, for all working regimes, placement of the thermocouples in the FB furnace, (left)

Numerical simulation of the penetration of a jet with liquid fuel and water into the FB

On the basis of the presented experimental results, it can be concluded that water in the fuel increases the global reaction rate of combustion in the FB furnace, where fuel is laterally fed into the bed. This phenomenon is associated with sudden transition of water in the fuel to steam

while entering the heated FB (≈ 900 °C), which causes the expansion of the input jet and better mixing of fuel with oxidizer (air), as well as breaking of liquid (still not vaporized) fuel into small droplets and increasing of the fuel's contact surface area with the environment. This phenomenon was observed both with light and heavier volatile liquid fuels (more and less evaporative liquid fuels, respectively), where for light volatile fuels, the effect of better mixing of volatiles from the fuel and the oxidizer, due to the rapid transition of water into steam and the expansion of the input jet, is more pronounced than the effect of breaking up the liquid fuel into small drops. This chapter presents the results of numerical experiments performed using Fluent's granular model of the FB, in order to verify the assumptions about the effect of better mixing of fuel volatile matter with the oxidizer when non-conventional fuel, which contains a substantial amount of moisture, is fed into the fluidization furnace.

Description of the model of feeding of non-conventional liquid fuel into heated FB

For numerical simulation of the penetration of a horizontal air/liquid fuel jet into the FB, Fluent's Euler-Euler granular model of the fluidized bed was used. The model governing and constitutive equations of penetration of one-component, isothermal jet have been presented in the subsection Euler-Euler granular model of the fluidized bed (eqs. 6-9). However, in the case of simulation of fuel and water jet penetration into the FB, this set of equations should be supplemented with transport equations of conservation of chemical components, and with the energy equation, which can be presented as:

– conservation equations for chemical components

$$\frac{\partial}{\partial t}(\alpha_g \rho_g Y_i) + \nabla(\alpha_g \rho_g \vec{v}_g Y_i) = \nabla(\alpha_g \rho_g D_{i,m} \nabla Y_i) + R_i \tag{11}$$

– energy equation

$$\frac{\partial}{\partial t}(\alpha_g \rho_g c_{p,g} T_g) + \nabla(\alpha_g \rho_g \vec{v}_g c_{p,g} T_g) = \nabla\left(\frac{k_t}{c_{p,g}} \nabla T_g\right) + \nabla(\sum_i \alpha_g \rho_g D_{i,m} c_{p,i} T_g \nabla Y_i) \tag{12}$$

It should be noted that this is a quasi-three-phase system: water in liquid state, gases with steam, and particles, with the assumption that the fuel evaporates instantly. Practically the fuel at the nozzle outlet is seen as a mixture of liquid (water) and gaseous volatile components. The numerical system is not really a three-phase one, since equations for only two phases are used: the fluid phase, consisting of liquid fuel/water with gases (water vapour, volatiles and air) and the particle phase, which consists of granular – bed particles.

Kinetics of water evaporation at the entrance into the FB is defined in analogy with the model of homogeneous chemical reactions, by using the Arrhenius expression for the reaction rate constant [25]: $R_{H_2O} = k_{o,1}\exp(-E_a/RT_g)\{H_2O\}$, where the pre-exponential factor is $k_{o,1} = 2.239$ and the activation energy is $E_a = 1 \cdot 10^6$ J/kmol.

A schematic view of the geometry of a numerically simulated fluidization reactor has already been shown in fig. 2, where the bed width and height (hatched area) were 0.3 m and 0.4 m, respectively. Modeled granular bed consists of particles with the diameter of 0.8 mm and density of 2600 kg/m^3, which were fluidized by heated air (at 1200 K) with the fluidization degree of 3. The temperature of the fuel/air mixture in the feeding jet is 300 K.

Calculations are non-stationary with a time step of $1.25 \cdot 10^{-4}$ s, with the total simulation time, determined on the basis of the time required for the passage of fluid through the space

occupied by the FB, so that a numerical simulation is monitoring the development of the jet in the bed.

The results of the numerical simulation of light volatile fuel feeding into the fluidization furnace

In this case the horizontal jet, which enters at room temperature into a heated fluidized bed, consists of air, liquid water (which, after mixing with heated FB, transforms into steam) and volatile fuel components. Volatile components have been simulated by propane, which in all numerical experiments entered into FB with the mass flow rate of 0.007453 kg/s. The total mass flow rate of air (air in the nozzle + air for fluidization) in all numerical experiments was the same as well (0.11627 kg/s), so that the overall fuel-air ratio is constant for all calculations. Only the portion of water in the fuel feeding nozzle flow changed, and in this way the influence of moisture content of a fuel on mixing intensity of volatiles and oxygen from the air was analyzed.

A series of calculations, for both the case when the fuel does not contain moisture and the case when it does, has been performed, whereas the values of mass fraction of moisture in the fuel ranged between 0.1 and 0.6. Figure 7 shows the simulation results of mass fraction distribution of volatiles within the jet penetration (after 0.057 s) for the case when the fuel does not contain water, fig. 7(a) and when the mass fraction of moisture in the fuel is 0.4, fig. 7(b). The presented results show that the zone of mixing of the volatiles with other components (including oxygen) was significantly wider in the case of feeding a fuel with moisture.

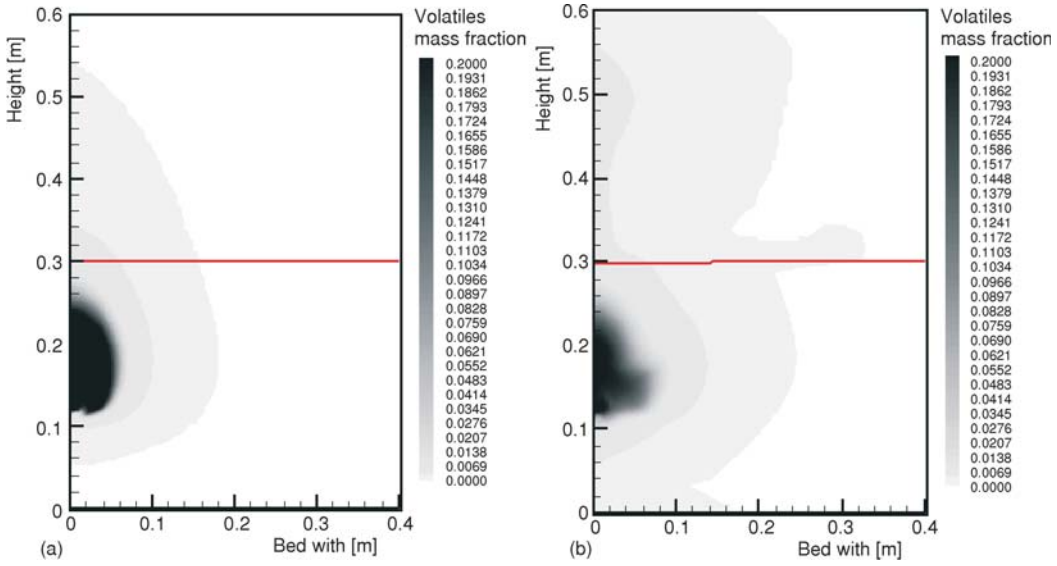

Figure 7. Distribution of the mass fraction of the fuel phase (propane) in the FB while fuel is fed without (a) and with water (b)

In order to quantitatively determine the influence of water content in the fuel on interfusion of the volatiles and oxygen from the fluidization air, the calculation for processing the obtained component concentrations fields at the end of the simulation process of jet development was applied. With this aim, statistical processing of results of non-stationary calculation by specially written subroutines in "C" language has been used.

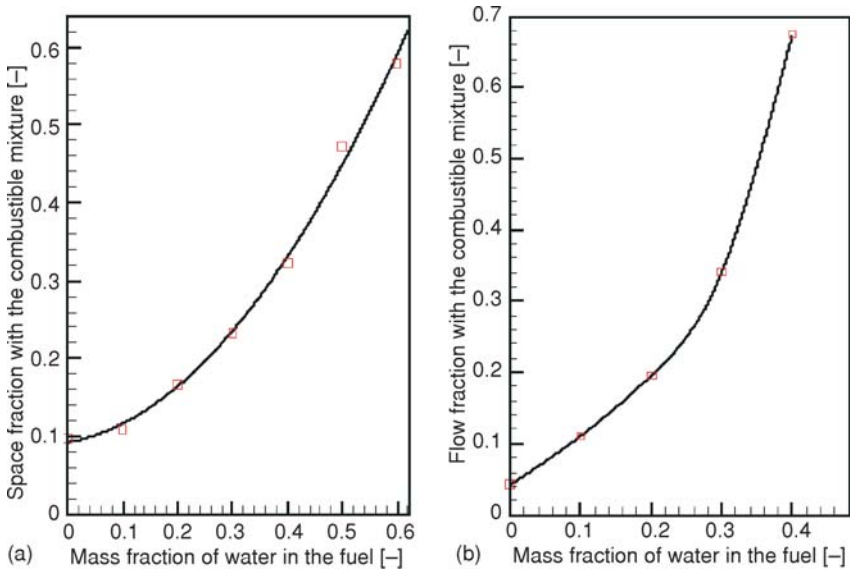

Figure 8. The portion of (a) the space with combustible fuel-air mixture and (b) the flow of the combustible fuel-air mixture, depending on the water mass fraction in the fuel

The results were analysed in two ways, *i. e.* when monitored parameter was: (a) the ratio of the number of control volumes, wherein the oxygen-to-fuel ratio is greater than or equal to stoichiometric, and of the total number of control volumes in the FB; (b) the ratio of the mass flow rate of the fluid that enters into the zone at the top of the FB, wherein the ratio of the fuel and oxygen is greater or equal to the stoichiometric, and of the total fluid mass flow rate that enters the zone at the top of FB.

In the diagrams shown in fig. 8, a quantitative indicator is presented, showing the influence of water content in the jet on the effect of mixing of fuel volatiles with oxygen from the fluidization air, after the period of jet development in the FB. Diagrams 8(a) and 8(b) correspond to the above mentioned models of analysis of results of numerical simulation (a) and (b), respectively. Both ways of analyzing the results of numerical simulations of horizontally fed fuel into the FB show that increased water content in the fuel jet increases the share of the space (*i. e.* the share of the flow) of the fuel-air mixture in the FB, which clearly shows that the portion of water in the fuel, which is fed into a heated FB, promotes the effect of mixing the fuel and oxidizer.

The results of the numerical simulation of heavy volatile fuel feeding into the fluidization furnace

In the case of heavy volatile liquid fuel (HVLF) feeding, the horizontal jet, which enters at room temperature into a heated fluidized bed, consists of air, water in liquid state (which, after mixing with heated FB, transforms into steam) and heavy volatile liquid oil. Non-conventional HVLF has been simulated by engine-oil, which does not significantly evaporate during jet development. Liquid fuel in all numerical experiments entered into FB with the flow rate of 0.007759 kg/s, while the total mass flow rate of air in all numerical experiments was 0.11627 kg/s.

In fig. 9 the simulation results of the gas volume fraction distribution (bed porosity) in the fluidizing reactor, with feeding of HVLF with and without moisture content, is given. The distribution of the porosity after an initial period of forming the jet, under the aforementioned

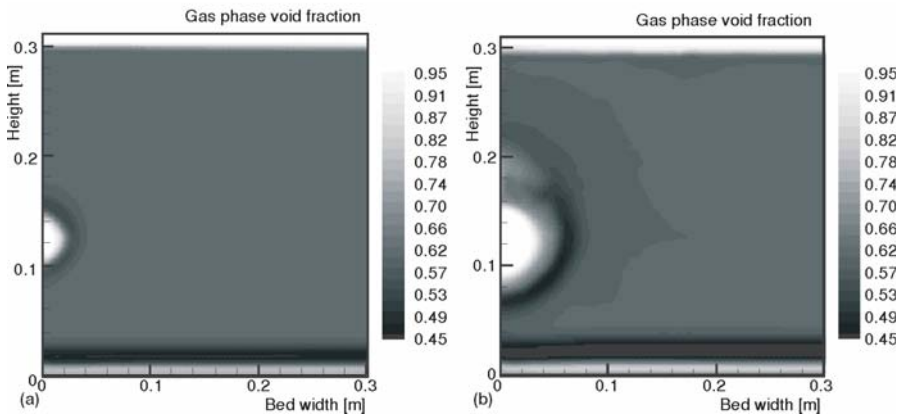

Figure 9. A change of bed porosity during the introduction of HVLF without water content (a) and in the introduction of HVLF mixed with water (water mass fraction in the fuel of 60%) (b)

conditions, is clearly shows that the water in the fuel affects jet penetration expansion during fuel feeding.

For the case of heavy volatile fuel feeding into the FB, also a series of numerical experiments has been performed, with fuel containing mass fraction of moisture in the range between 0.1 and 0.6. Figure 10 shows the simulation results of engine-oil mass fraction distribution during feeding of liquid fuel, after jet development time (0.05 s). Two cases were considered: when the fuel does not contain water, fig. 10(a), and when the mass fraction of moisture in the fuel is 0.6, fig. 10(b). Gray areas in fig. 11 are areas containing a combustible mixture of oil and oxygen, and the black zone corresponds to stoichiometric relation of fuel and oxygen, while the white area corresponds to very low concentrations of fuel. The presented results show that the

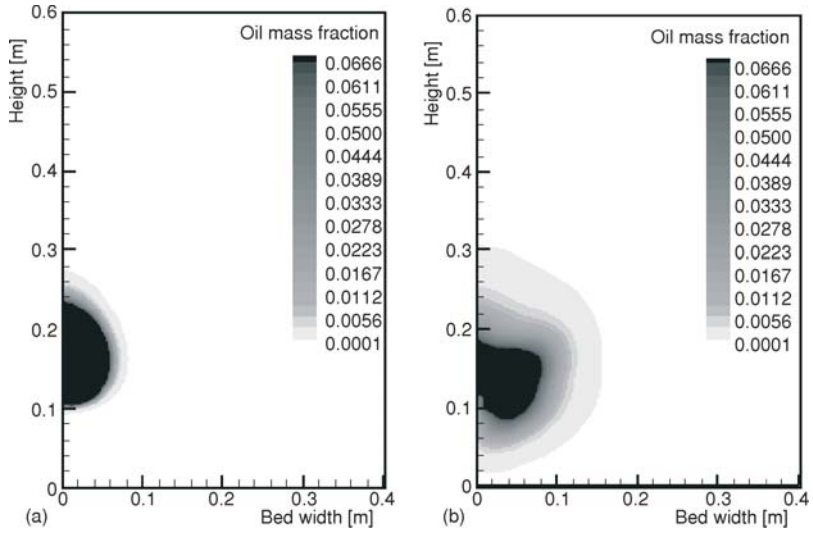

Figure 10. The mass fraction distribution of engine-oil in the FB feeding fuel without (a) and with water (b)

zone of combustible mixture of oil and oxygen was significantly higher in the case of feeding a fuel with moisture.

In the diagram shown in fig. 11, a quantitative indicator is presented, showing the influence of water content in the jet on the effect of mixing heavy volatile fuel with oxygen from the fluidization air, after the period of jet development in the FB. The quantitative indicator is based on the monitoring of the ratio of the number of control volumes, wherein the oxygen-to-fuel ratio is greater than or equal to stoichiometric, and of the total number of control volumes in the FB (as it is explained in the previous chapter). Presented analyses of results show that increased water content in the heavy volatile liquid fuel, fed directly into the FB, increases the share of the space of the combustible fuel-air mixture in the FB. This clearly shows that the portion of water in the liquid fuel, which is fed into a heated FB, enhances the effect of mixing the fuel and oxidizer.

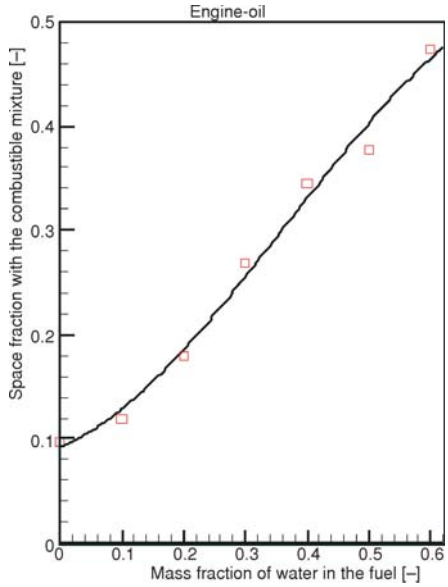

Figure 11. The portion of the space with combustible fuel-air mixture *vs.* water mass fraction in the fuel

Conclusions

The paper presents two 2-D CFD models of the FB, based on two-fluid FB simulation procedure. The proposed fluidization models have been verified by comparing their results with a number of experimental results from the literature, applied for the analysis of horizontal jet penetration into a 2-D FB fluidized bed.

In addition, numerical experiments were performed using Fluent's FB granular model to analyze the effect registered in the experiments in a pilot fluidization furnace with liquid fuels feeding into the bed, when some withdrawal of the intense combustion zone towards the bed bottom was noticed, during the combustion of liquid fuels with significant water content, compared to fuel with less moisture content. This leads to the conclusion that the water in the fuel improved mixing of fuel and oxidizer which indirectly increases the global reaction rate of combustion in the FB furnace.

In order to analyze this phenomenon, two series of numerical experiments were performed: when light volatile liquid fuel was fed into the FB, and when heavy volatile oil was fed into a heated FB. Specifically, a series of calculations of jet penetration was done, where the jet included air, volatiles, or heavy volatile liquid fuel and water in liquid state, which, after entering the heated FB, turns into steam. The kinetics of water evaporation at the entry into the FB has been defined in analogy with the model of homogeneous chemical reactions, with the application of the Arrhenius expression for the constant of the reaction rate for the change of phase. Numerical simulation of both cases of horizontal feeding of liquid fuel into the fluidization furnace show that the water content in the fuel stream increases the share of space, *i. e.* the share of the flow of the combustible fuel-air mixture, from which it can be concluded that the water in the fuel promotes the mixing effect of fuel and oxidizer in the zone immediately after the feeder. Moreover, the simulations show that the water in the fuel affects the extension of the gas phase volume fraction, and thus the expansion of feeding jet penetration.

The presented results might be of practical importance for optimization of different liquid fuels combustion in the FB furnace, especially non-conventional fuels such as oil sludge and waste materials, the combustion of which can be intensified by injecting a proper mixture of fuel and water.

Acknowledgment

The authors wish to thank the Serbian Ministry of Education, Science and Technological Development for financing the project "Improvement of the industrial fluidized bed facility, in scope of technology for energy efficient and environmentally feasible combustion of various waste materials in the fluidized bed" (Project TR33042).

Nomenclature

C_D – drag coefficient, [–]
$c_{p,g}$ – gas specific heat capacity, [kJkg^{-1}K^{-1}]
$D_{i,m}$ – mass diffusion coefficient for species i, [m^{2}s^{-1}]
d_j – nozzle opening diameter, [m]
d_p,d_s – particle mean diameter, [m]
e_s – restitution coefficient, [–]
g – gravity acceleration, [ms^{-2}]
g_{0s} – radial distribution function, [–]
H_2O – water concentration, [%]
[I] – unit tensor, [–]
$\mathbf{I}_{2D}$ – second invariant of deviatoric stress tensor, [–]
$K_{1,i}$ – laminar flow permeability in i direction, [m^2]
$K_{2,i}$ – turbulent flow permeability in i direction, [m]
K_{GS} – gas/solid momentum exchange, [–]
k – turbulent kinetic energy, [m^{2}s^{-2}]
k_t – thermal conductivity, [Wm^{-1}K^{-1}]
$k_{\theta s}$ – granular energy diffusion coefficient, kgm^{-1}s^{-1}]
L_j – jet penetration length, [m]
p – pressure, [Pa]
R – universal gas constant, [Jmol^{-1}K^{-1}]
R_{H_2O} – evaporation rate, [–]
$\mathbf{S}_k$ – strain rate tensor, [s^{-1}]
T – absolute temperature, [K]
U_j – velocity at the nozzle outlet, [ms^{-1}]
U_j, U_i – vectors of fluid average velocity, [ms^{-1}]
U_{MF} – minimum fluidization velocity, [ms^{-1}]
U_s – gas velocity at a free cross-section above the bed, [ms^{-1}]
$\vec{u}$ – instantaneous velocity vector, [ms^{-1}]
V – volume, [m^3]
X_i, X_j – co-ordinates, [m]
Y_i – species mass fraction, [–]

Greek symbols

α_k – phase void fraction, [–]
$\gamma_{\Theta s}$ – collisional dissipation energy, [kgs^{-3}m^{-1}]
ε – turbulent kinetic energy dissipation, [m^{2}s^{-3}]
Θ_s – granular temperature, [m^{2}s^{-2}]
λ – bulk viscosity, [kgm^{-1}s^{-1}]
μ – dynamic viscosity, [kgm^{-1}s^{-1}]
μ_{eff} – effective dynamic viscosity, [kgm^{-1}s^{-1}]
$\mu_{s,coll}$ – collisional viscosity, [kgm^{-1}s^{-1}]
$\mu_{s,fr}$ – frictional viscosity, [kgm^{-1}s^{-1}]
$\mu_{s,kin}$ – kinetic viscosity, [kgm^{-1}s^{-1}]
μ_t – dynamic turbulent viscosity, [kgm^{-1}s^{-1}]
ρ – fluid density, [kgm^{-3}]
τ – phase stress-strain tensor, [Pa]
ϕ – angle of particle internal friction, [–]
ϕ_{gs} – kinetic energy transfer rate, [kgs^{-3}m^{-1}]
ψ_{fr} – effective friction coefficient, [–]

Subscripts

b – fluidized bed
g – gas
s – solid/granular phase

References

[1] Saxena, S. C., Jotshi, C. K., Fluidized Bed Incineration of Waste Materials, *Progress in Energy and Combustion Science, 20* (1994), 4, pp. 281-324, DOI: 10.1016/0360-1285(94)90012-4
[2] Link, J. M. *et al*., Flow Regimes in a Spout-Fluid Bed: A combined Experimental and Simulation Study, *Chemical Engineering Science, 60* (2005), 13, pp. 3425-3442
[3] Utikara, R. P., Ranade, V. V., Single Jet Fluidized Beds: Experiments and CFD Simulations with Glass and Polypropylene Particles, *Chemical Engineering Science, 62* (2007), 1-2, pp. 167-183, DOI: 10.1016/j.ces.2006.08.037

[4] Di Renzo, A., Di Maio, F. P., Homogeneous and Bubbling Fluidization Regimes in DEM-CFD Simulations: Hydrodynamic Stability of Gas and Liquid Fluidized Beds, *Chemical Engineering Science, 62* (2007), 1-2, pp. 116-130, DOI: 10.1016/j.ces.2006.08.009
[5] Enwald, H., *et al*., Simulation of the Fluid Dynamics of a Bubbling Fluidized Bed, Experimental Validation of the Two-Fluid Model and Evaluation of a Parallel Multiblock Solver, *Chemical Engineering Science, 54* (1999), 3, pp. 311-328 DOI: 10.1016/S0009-2509(98)00186-9
[6] Nemoda, S., *et al*., Numerical Model of Gaseous Fuel Jet Injection into a Fluidized Furnace, *International Journal of Heat and Mass Transfer, 52* (2009), 15-16, pp. 3427-3438, DOI: 10.1016/j.ijheatmasstransfer.2009.02.045
[7] Hong, R., *et al*., Studies on the Inclined Jet Penetration Length in a Gas-Solid Fluidized Bed, *Powder Technology, 92* (1997), 3, pp. 205-212
[8] ***, *Fluidization*, 2nd ed. (Eds. J. F. Davidson, R. Cliff, D. Harrison), Academic Press, London, 1985
[9] Patankar, S. V., *Numerical Heat Transfer and Fluid Flow*, Hemisphere, New York, USA, 1980
[10] Patankar, S. V., Spalding, D. B., A Calculation Procedure for Heat, Mass and Momentum Transfer in Three-Dimensional Parabolic Flows, *Int. Journal of Heat and Mass Transfer, 15* (1972), 10, pp. 1787-1806 DOI: 10.1016/0017-9310(72)90054-3
[11] Vejahati, F., *et al.*, CFD Simulation of Gas-Solid Bubbling Fluidized Bed: A New Method for Adjusting Drag Law, *Can. J. Chem. Eng., 87* (2009), pp. 19-30
[12] Syamlal, M., *et al*., MFIX Documentation Theory Guide, U. S. Department of Energy, Office of Fossil Energy Morgantown Energy Technology Center, Morgantown, W. Va., USA, 1993
[13] Lun, C. K. K. *et al.*, Kinetic Theories for Granular Flow: Inelastic Particles in Couette Flow and Slightly Inelastic Particles in a General Flow Field, *Journal of Fluid Mechanic., 140* (1984), pp. 223-256, DOI: 10.1017/S0022112084000586
[14] Schaeffer, D. G., Instability in the Evolution Equations Describing Incompressible Granular Flow, *J. Diff. Eq., 66* (1987), 1, pp. 19-50, DOI: 10.1016/0022-0396(87)90038-6
[15] Syamlal, M., O'Brien, T. J., Simulation of Granular Layer Inversion in Liquid Fluidized Beds, *International Journal of Multiphase Flow, 14* (1988), 4, pp. 473-481, DOI: 10.1016/0301-9322(88)90023-7
[16] Shakhova, N. A., Discharge of Turbulent Jets into a Fluidized Bed, *Journal of Engineering Physics and Thermophysics, 14* (1968), 1, pp. 32-36
[17] Zenz, F. A., Bubble Formation and Grid Design, *IChemE Symposium Series, 30* (1968), pp. 136-139
[18] Merry, J. M. D., Penetration of a Horizontal Gas Jet into a Fluidised Bed, *Transactions of the Institution of Chemical Engineers and the Chemical Engineer, 49* (1971), 4, pp. 189-195
[19] Kozin, B. E., Baskakov, A. P., Studies on the Jet Range in a Bed of Granular Particles, *Khim I Teckhnol Topliv I Masel, 3* (1967), pp. 4-7
[20] Yates, J. G., *et al*., Particle Attrition in Fluidized Beds Containing Opposing Jets, *AIChE Symp. Ser., 281* (1988), pp. 13-19
[21] Benjelloun, F., *et al*., *Penetration Length of Horizontal Gas Jets into Atmospheric Fluidized Beds*, Proc. Fluidization-VIII (Eds. J.-F. Large, C. Laguerie,), Engineering Foundation, N.Y., USA, 1995, pp. 239-246
[22] Mladenović, M. R. *et al*., Vertical Temperature Profile in the Installation for the Combustion of Waste Fuels in the Fluidized Bed Furnace, *Proceedings on CD-ROM,* 15th Symposium on Thermal Science and Engineering of Serbia, Sokobanja, Serbia, 2011, ISBN 978-86-6055-018-9, pp. 490-499
[23] Mladenović, M. R., *et al*., Vertical Temperature Profile in the Installation for the Combustion of Waste Fuels in the Fluidized Bed Furnace (in Serbian), *Termotehnika, XXXVIII* (2012), 1, pp. 11-24
[24] Mladenović, M. R., *et al*., Combustion of Low Grade Fractions of Lubnica Coal in fluidized bed, *Thermal Science, 16* (2012), 1, pp. 297-311
[25] Brennan, J. F., Shapiro, J. S., Watton, E. C., Evaporation of Liquids: A Kinetic Approach, *J. Chem. Educ., 51* (1974), 4, p. 276

Paper submitted: November 16, 2012
Paper revised: December 10, 2012
Paper accepted: December 24, 2012